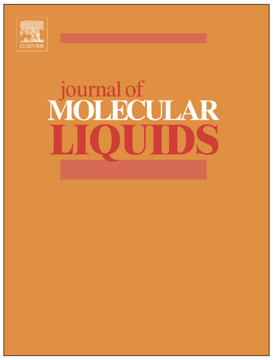

Self-assembly of taper- and wedge-shaped maleimide derivatives: Synthesis and structure-property relationship

D.R. Vinayakumara, Sandeep Kumar, S. Krishna Prasad, Airody Vasudeva Adhikari

PII: S0167-7322(18)35350-9
DOI: https://doi.org/10.1016/j.molliq.2019.02.054
Reference: MOLLIQ 10455

To appear in: *Journal of Molecular Liquids*

Received date: 16 October 2018
Revised date: 28 January 2019
Accepted date: 10 February 2019

Please cite this article as: D.R. Vinayakumara, S. Kumar, S.K. Prasad, et al., Self-assembly of taper- and wedge-shaped maleimide derivatives: Synthesis and structure-property relationship, Journal of Molecular Liquids, https://doi.org/10.1016/j.molliq.2019.02.054

Self-assembly of Taper- and Wedge-Shaped Maleimide Derivatives: Synthesis and Structure-property Relationship

D. R. Vinayakumara,[a] Sandeep Kumar, [b] S. Krishna Prasad,[c] Airody Vasudeva Adhikari.*[a]

[a] Organic Materials Laboratory, Department of Chemistry, National Institute of Technology Karnataka, Surathkal, Mangalore 575 025, India.

[b] SCM group, Raman Research Institute, C.V. Raman Avenue, Sadashivanagar, Bangalore - 560 080, India.
[c] Centre for Nano and Soft Matter Sciences, Jalahalli, Bangalore-560 013, India.

Corresponding Author: Airody Vasudeva Adhikari

E mail: avachem@gmail.com; avachem@nitk.ac.in

Abstract

Herein, we describe design and synthesis of five new amphiphilic systems, *viz*. **10b-c** and **11a-c** composed of maleimide at the focal point and alkoxy phenyl ring at the periphery. Their self-assembling behaviour was examined systematically by varying the length of hydrophobic part and aromatic core segment. Evidently, on increasing the aromatic core length, maleimide based amphiphiles relatively emerge as two distinct molecular structures, *i.e.* wedge- and tapered-shaped. The mesomorphic studies of the two series reveal that, tapered-shaped maleimide derivatives assemble into a smectic A phase with an interesting phasmidic arrangement, whereas the wedge-shaped molecules exclusively form a prospective supramolecular hexagonal columnar mesophase through the intermolecular hydrogen-bonding *via* maleimide head group. These self-assembled materials could demonstrate high-sensitivity towards various external stimuli.

Keywords

Supramolecular chemistry; Amphiphiles; Hydrogen bonding; Heterocycles; Thermotropic liquid crystals

1. Introduction

In this advanced era, novel liquid crystalline (LC) materials are being successfully employed in the wide range of fields from electronics to biomedical, because of their unique properties [1–6]. In fact, LCs are regarded as “soft matters” which possess molecular order, yet fluidic assemblies by the dint of variety of non-covalent interactions. Now, supramolecular liquid crystals are considered to be fascinating soft materials, wherein small molecular components associate to form complex nanoscale architectures through interactions such as hydrogen bonding, dipolar interactions, Coulombic forces, π-π interactions, metal complexation, ionic attentions or combination of these [7–9]. These nanosegregated structures are highly dynamic, their properties are typically depending on the nature of constituent building blocks as well as the type of forces by which they assembled. Such mesogens are promising functional materials in numerous applications mainly due to their high response towards the external stimuli [10–19].

Recently, liquid crystals formed through hydrogen-bonding interaction have attracted intense scientific attention in the area of soft materials [20–26]. Generally, the mode of H-bonding in LCs can be divided into close-type and open-type. The former type of H-bonding generates closed complexes, while the latter leads to form ribbon or layer kind of structures [9]. Till now, a number of H-bonded motifs such as heterocycles, polyalcohols, carboxylic acids, amides, amines and properly functionalized carbonyl structures, have been used to obtain supramolecular liquid crystals [27]. Amid, heterocyclic systems are of particular importance due to their ability of forming stable and specific H-bonds, imparting lateral and longitudinal dipoles to overall structure [9]. Moreover, electron deficient nature of heterocycles impel the important electronic communication throughout the structure when they appended with electron donating moieties. This feature also provides a good optoelectronic property to the molecules, such materials can potentially be used as active components in OLEDs, solar cells, TFT, *etc* [11].

In the literature, heterocycles capable of forming H-bonding such as pyridone [28], melamine [24,29], 1H-pyrazole [21,23,30], barbituric acid [31,32], folic acid [33–35], 1H-imidazole [36–38] and some factionalized heterocycles [22,39–41] have been reported as potential structural motifs to achieve supramolecular liquid crystals. In this context, we recently explored cyanopyridone as an eminent electron deficient motif with proper donor-acceptor configuration to realize the luminescent liquid crystalline material for OLED application [42–45]. In continuation of our effort on finding different heterocyclic systems for developing the various functional liquid crystalline materials, herein we report two new series of maleimide based LCs carrying trialkoxy phenyl rings. The two different taper and wedge-shaped amphiphiles, exhibiting supramolecular LC behaviour have been designed, synthesized and characterized systematically to understand the structure-property relationship in view of their potential application in electronic devices (Figure 1).

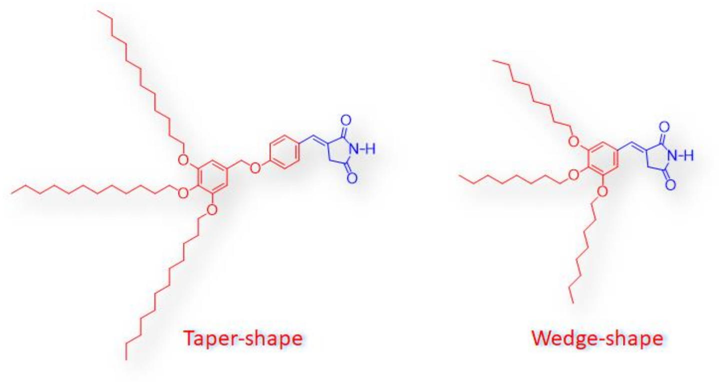

Figure 1. Newly designed amphiphilic LCs

2. Results and discussion

2.1 Synthesis and characterization

The synthetic route for the preparation of newly designed maleimide derivatives is described in Scheme 2. The required key-precursors, *i.e.* trialkoxy benzyl bromides, **5b-c** [46] and trialkoxy benzaldehydes, **6a-c** [47] were synthesized by adopting well-documented procedures with optimized conditions (Scheme 1). Synthesis of first series of targeted compounds **10b-c** involves a simple O-alkylation of 4-hydroxybenzaldehyde (**7**) with **5b-c**, followed by the Wittig condensation of aldehydes **8b-c** with maleimide derivative **9**, which was prepared by the Michael addition reaction of triphenylphosphine to maleimide. Further, trialkoxybenzylidenyl maleimides **11a-c** were obtained by using Wittig's protocol. The reaction, under the reflux condition in methanol, yielded the desired product with an (*E*)-configuration exclusively (yield of 40-60 %). The structures of the newly synthesized compounds were determined by FTIR, ^{1}H-NMR, ^{13}C-NMR spectral and elemental analyses.

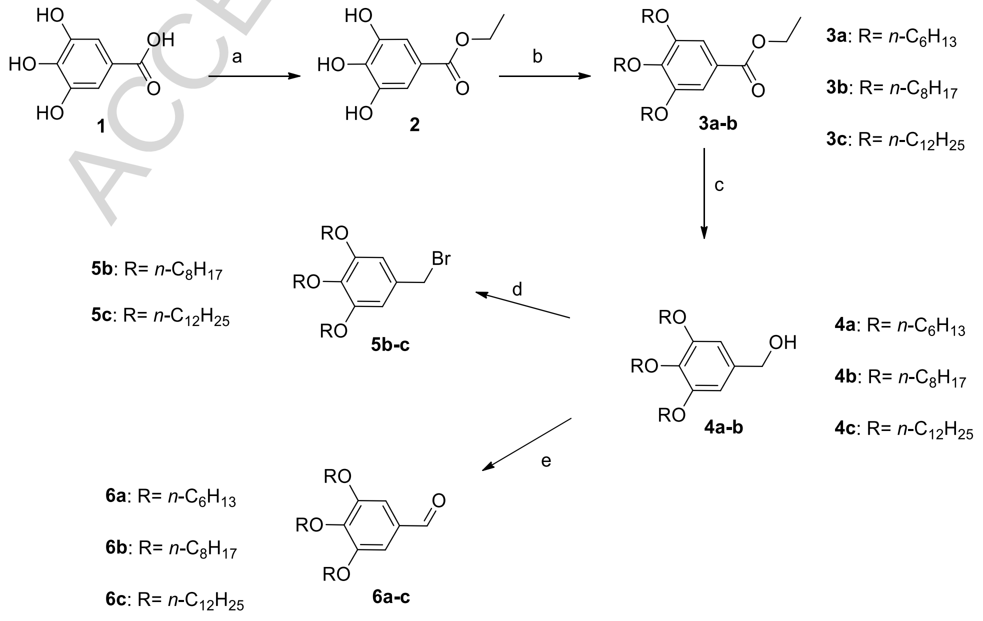

Scheme 1. Synthesis of key-intermediates. Reagents and conditions: (a) Cat. H_2SO_4, EtOH, reflux, overnight, 89 %; (b) *n*-alkylbromide, K_2CO_3, KI, DMF, 80 ℃, 12 hrs, 71-85 %; (c) $LiAH_4$, anhydrous THF, 0 ℃, 15 hrs, 86-90 %; (d) PBr_3, dry DCM, 4 hrs, 70-85 %; (e) PCC, dry DCM, 3 hrs, 63-86 %

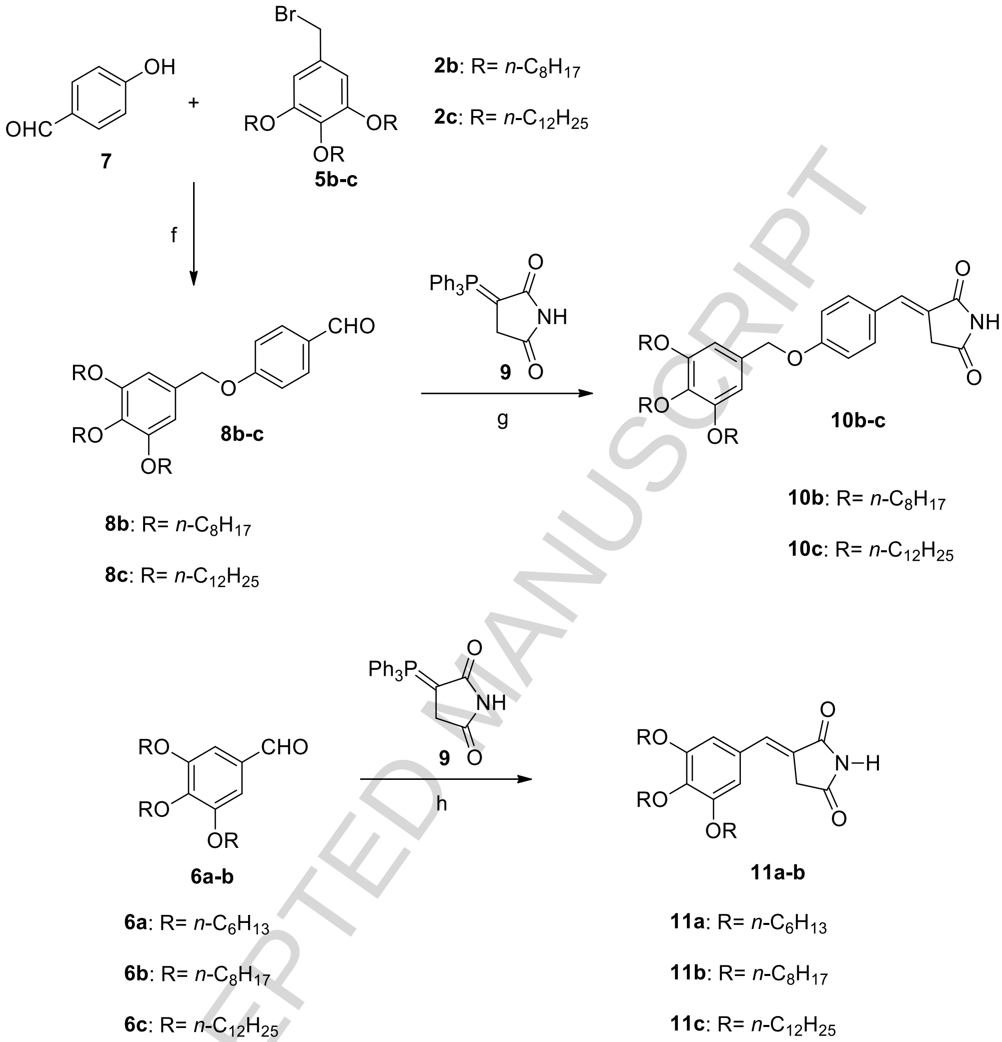

Scheme 2. Synthesis of maleimide derivatives. Reagents and conditions: (f) K_2CO_3, DMF, 70 ℃, overnight, 78-81 %; (g) CH_3OH, reflux, 10 hrs, 45-40 %; (h) CH_3OH, reflux, 10 hrs, 51-60 %

2.2 Experimental methods

General procedure for the synthesis of precursor aldehydes, ***8b-c***

A mixture of 4-hydroxybenzaldehyde (**7**) (1 equiv.), trioctyloxybenzyl bromide (**5a**) (1.1 equiv.) and anhydrous K_2CO_3 (2 equiv.) in 10 volume of dry DMF was heated to 70 ℃ under an argon atmosphere for overnight. Then, the mixture was poured into ice cooled water and the obtained precipitate was filtered. The crude was recrystallized from cold methanol to get the pure product.

*General procedure for the synthesis of target compounds **10b-c** and **11a-b***

An equimolar mixture of aldehyde (1 equiv.) and triphenylphosphoranylidenyl succinimide (**9**) (1 equiv.) in 10 volume of methanol was reflexed for 10 hrs. After completion of the reaction, the mixture was allowed to cool at room temperature. The obtained white precipitate was filtered and washed with methanol. Then, the crude was purified by silica gel column chromatography (100-200 mesh size) eluting with a mixture of ethyl acetate and pet-ether (60-70 ℃) to yield final compounds.

2.3 Self-assembling properties

The self-assembling behaviour of newly synthesized compounds was systematically studied by using DSC, POM and XRD analytical techniques. The thermal properties were investigated by DSC scan at the rate of 5 ℃/min under a nitrogen atmosphere. The compound, **10b** bearing triple octyloxy chains showed two distinct crystalline states, which clear at 100.21 ℃on heating. In cooling scan, a trivial transition peak was observed at 89.69 ℃with an enthalpy of -2.0 kJmol^{-1} which could be assigned to an I-LC transition and on further cooling, the compound has crystallized. In the DSC scan of longer chain analogue, *i.e.* **10c**, two endothermic peaks corresponding to Cr-Cr transition and a small LC-I transition (100.34 ℃) were observed. The mesophase was reappeared at 99.14 ℃ (-1.39 kJmol^{-1}) on cooling cycle and no sign of crystallization was noticed till room temperature.

The observed thermotropic transitions were further confirmed by polarized optical microscope and they were identified to be quite consistent with DSC results. As shown in Figure 2, both the compounds displayed birefringent pseudo focal-conic texture on slow cooling from their respective isotropic phase, which are commonly encountered textures for smectic A phases of calamitic and bent-core LC systems [25,48,49].

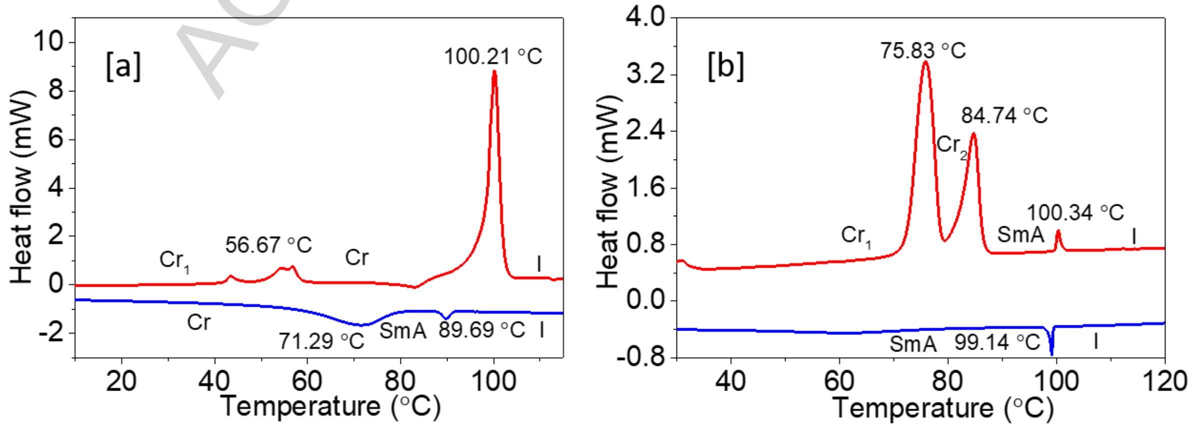

Figure 2. DSC thermograms of (a) **10b** and (b) **10c** recorded at a rate of 5 ℃/min under a nitrogen atmosphere (red and blue traces represent heating and cooling scans, respectively)

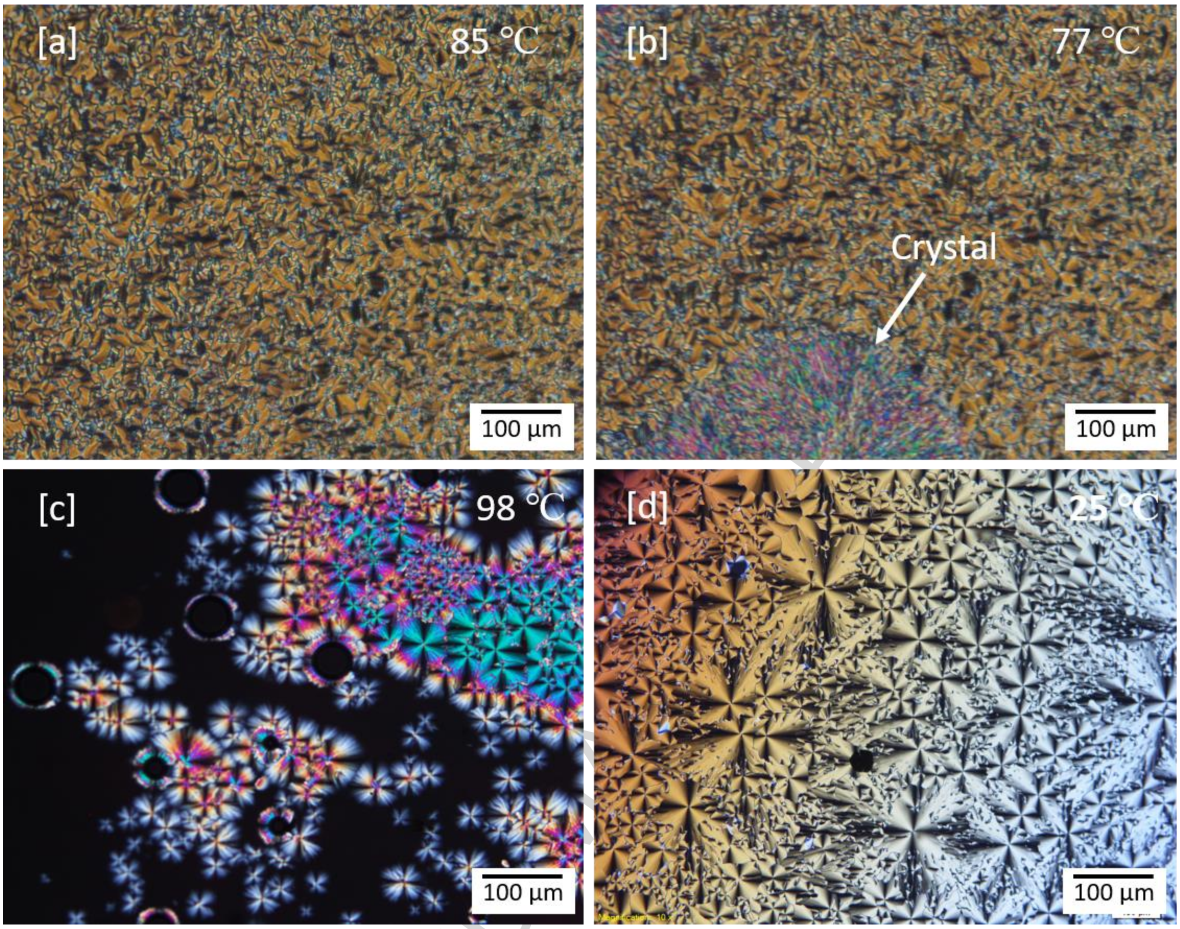

Figure 3. Microphotographs of **10b** captured on slow cooling at (a) 85 ℃ and (b) 77 ℃; textures of **10c** obtained at (c) 98 ℃ and (d) 25 ℃

Table 1. ^{a} Thermal transitions and associated enthalpy changes

Compd.	Phase sequence	
	Heating	Cooling
10b	Cr$_1$ 56.67 (4.97) Cr$_2$ 100.21 (45.24) I	I 89.69 (-1.20) Sm A ^{b} 71.29 (-16.60) Cr
10c	Cr$_1$ 75.83 (53.90) Cr$_2$ 84.74 (27.03) Sm A 100.34 (1.44) I	I 99.14 (-1.39) Sm A ^{c}
11a	Cr$_1$ 57.37 (22.78) Cr$_2$ 124.25 (29.89) I	I 115.39 (-29.42) Cr$_2$
11b	Cr$_1$ 63.22 (5.62) Cr$_2$ 124.16 (32.71) I	I 122.75 (-3.65) Col$_h$ ^{b} 112.76 (-28.28) Cr$_2$
11c	Cr$_1$ 33.38 (14.84) Cr$_2$ 118.42 (23.52) I	I 113.27 (-23.33) Cr$_2$ 30.60 (-16.67) Cr$_1$

[a] Peak temperatures/℃ (enthalpies/kJmol^{-1}) obtained by endothermic and exothermic cycles at the rate of 5 ℃/min; [b] monotropic mesophase; [c] Crystallization transition was not noticed till RT; Cr, Cr$_1$ and Cr$_2$, are different crystalline states; SmA = Smectic A mesophase; Col$_h$ = columnar hexagonal mesophase; I = isotropic liquid state

In order to get further insight into the molecular self-assembling in the smectic phase of taper-shaped amphiphilic systems, we recorded XRD spectra of **10c** at different temperatures throughout its LC phase range. The obtained spectra are depicted in Figure 4 and the relevant data are summarized in Table 2. At all the four temperatures, the XRD profile has evidently two common features: a sharp and intense peak at low angles and a diffuse broad one at wider angles. These features are typical of a layered smectic phase, a fact corroborated by POM textures. For further description we consider the profile at the lowest temperature, *i.e.* at T = 55 ℃, shown in Figure 4, as the additional features become more clear at this temperature. Three more peaks, one at low angles, sharp albeit very weak, a diffuse one at low angles and another diffuse peak at large angles, again weak. The identification of second reflection in the lower angle is easy since its spacing is exactly half of that of the fundamental (first reflection). Thus, it is the second harmonic, which is barely seen at T = 95 ℃, but picks up intensity as the temperature is lowered. The presence of another diffuse peak at the spacing ~16.5 Å is somewhat intriguing. In the light of the fact that, this value matches the longitudinal dimension of the core portion of the molecules, we propose that, the core regions of the neighbouring molecules completely overlap and the phasmidic chains stick out as the two termini of this dimer pair (Figure 5). Thus, the thickness of this partially interdigitated layer would be the dimension of the core plus the twice the length of terminal chain. With the length of 12-carbons being ~14 Å, the determined dimer length of 45 Å matches with the experimentally obtained layer thickness.

Since the bifurcation between the core and the hydrocarbon chain is better defined in the phasmidic arrangement, the overlapped core region can be considered to be a sub-layer, giving rise to its own X-ray diffraction. This results in the peak at ~16.5 Å, which is the dimension of the core. However, unlike the layer interfaces determined by the extreme ends of the dimer, there is enough liberation possible for the overlapped region of the core resulting in a spread of the diffraction pattern. The diffuse peak in higher angle region corresponding to ~3.42 Å, is commonly seen in columnar phases of discotic molecules. Except in systems wherein the terminal chains have different character, such as hydrocarbon/fluorocarbon or hydrocarbon/cholesteryl [50,51], it is not seen in smectic phases. Extending the argument made for the case of discotic systems, we propose that, peak spacing 3.42 Å arises due to the correlation between the core-parts of the neighbouring molecules. As expected, this correlation improves on lowering the temperature, and from the peak width, it is seen that, about 6 molecules are correlated. As observed commonly, increasing the layer spacing on lowering the temperature, owing to stretching of the chains (moving towards all-trans). However the consequent negative thermal expansion (d/dT) layer spacing of ~ 0.09 Å/℃ is quite large than usual smectics [52].

Table 2. XRD indexation of mesogen **10c**

Compound	d_{obs} [Å] at 25 ℃	d_{obs} [Å] at 55 ℃	d_{obs} [Å] at 75 ℃	d_{obs} [Å] at 95 ℃
10c	45.48 24.81 16.51 4.35 3.38	43.32 21.59 16.37 4.41 3.42	40.66 20.32 16.08 4.43	39.11 19.64 16.03 4.46

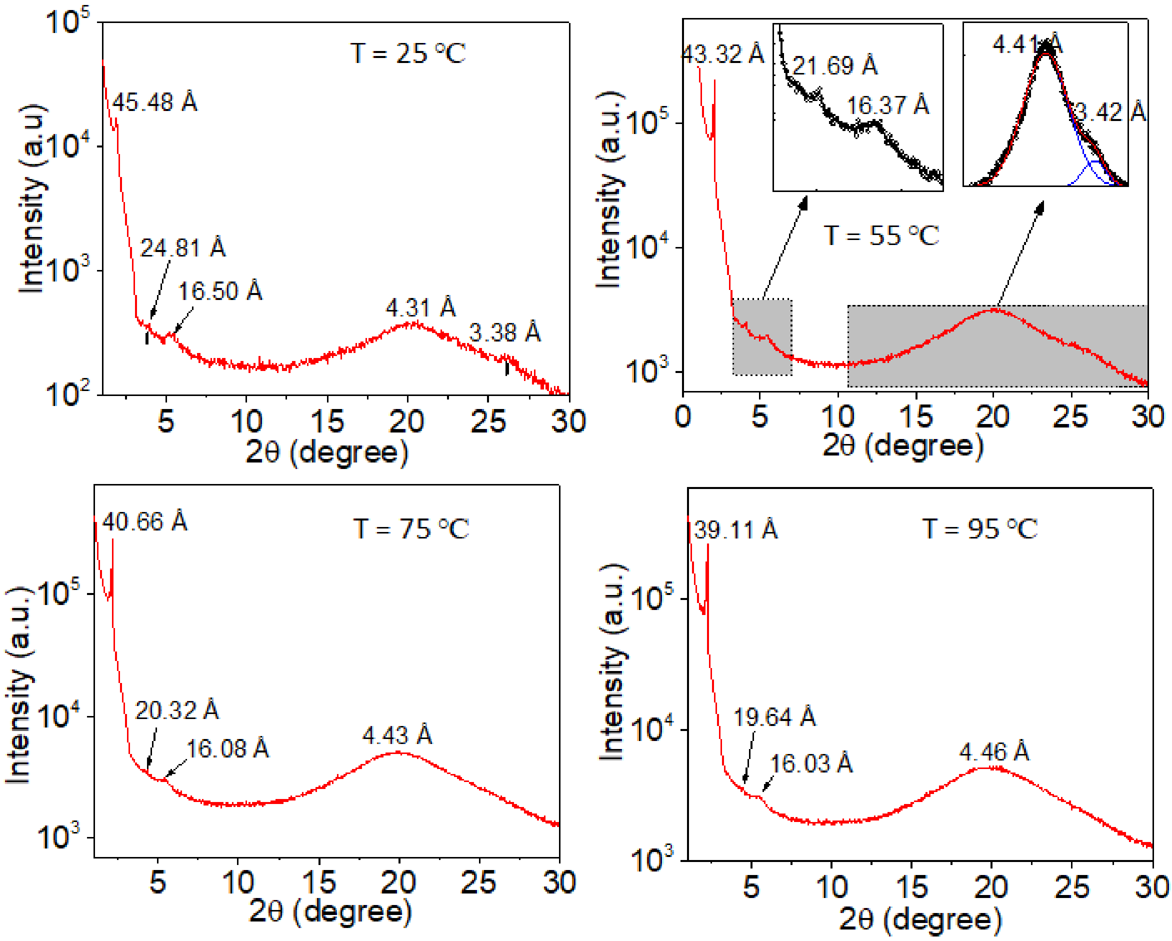

Figure 4. XRD pattern obtained for **10c** at various temperatures on cooling from I phase

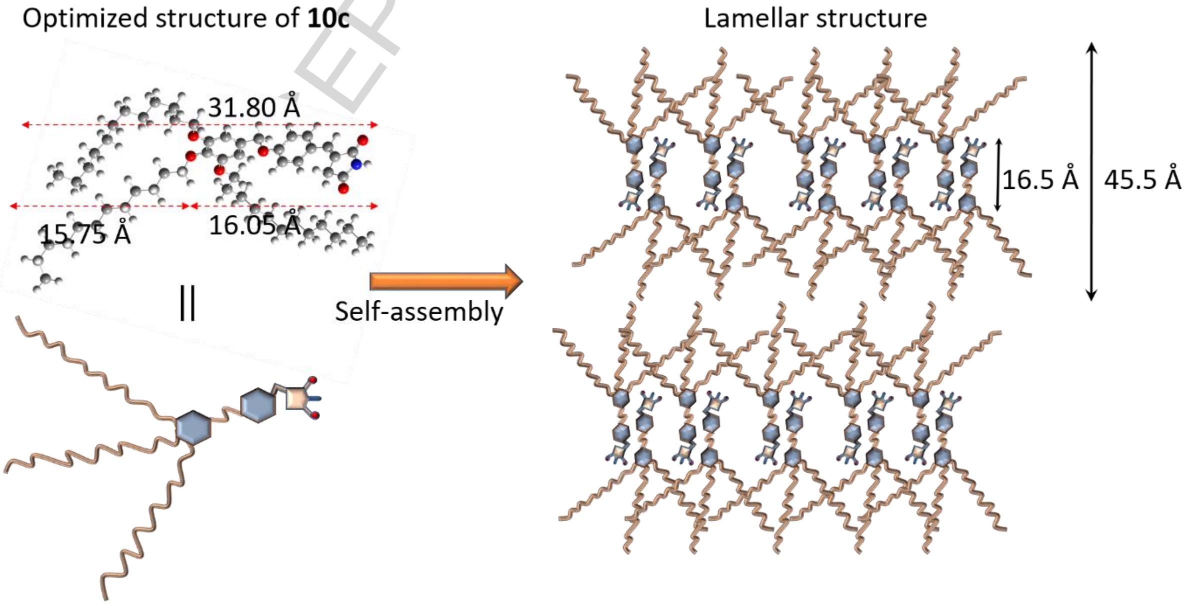

Figure 5. Schematic illustration of SmA mesophase structure of **10c**

On reducing the hydrophobic part in the design, we obtained a wedge configured molecules (**11a-c**), wherein three alkoxy groups attached to phenyl ring connected with polar maleimide ring. DSC traces of all the three compounds with varied aliphatic chain lengths reveal that, they exhibit polymorphic nature as a function of temperature (Figures S1-S2). Among them, the midst member, *i.e.* **11b** has shown a monotropic mesophase behaviour as apparent in its first cooling cycle of DSC scan, which was further confirmed by immediate reheating and cooling scans as shown in Figure 6b. Under POM, slow cooling from its I phase brings about a bright mosaic pattern which is a typical indication of presence of columnar organization (Figures 6c-d) [53].

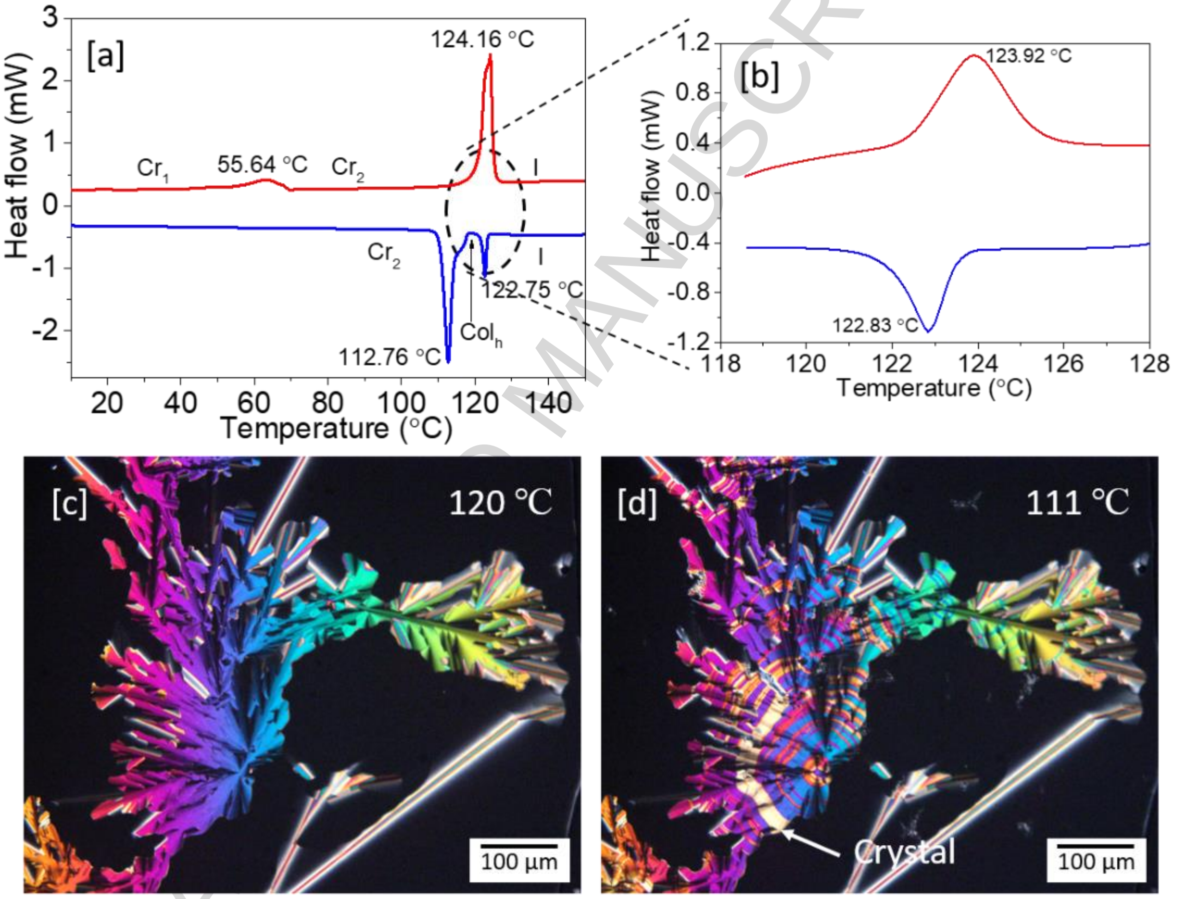

Figure 6. DSC traces of **11b:** (a) first heating and cooling scan (red and blue traces represent heating and cooling scans, respectively) and (b) second cycle; POM textures of **11b** captured at (c) at 120 °C and (d) 111 °C

To understand the structure of columnar mesophase of **11b**, we carefully recorded the XRD spectra within its short thermal range on slow cooling from I phase as depicted in Figure 7. For instance, the spectrum obtained at 125 °C displayed three reflections at the Bragg's d-spacings 27.57, 16.01 and 13.44 Å with the reciprocal ratio of 1: √3: 2 in the lower angle region.

In addition, a broad halo appears at wide angle region ascribed to liquid-like motion of the alkyl chains. The lower angle reflection could be index to (10), (11), (20) planes of two dimensional hexagonal geometry with the lattice parameter $a = 31.83$ Å. Further, the number of molecules (Z) occupied in each hexagonal unit cell was estimated using the XRD results, assuming the density value for these molecules is 1 gcm^{-3} [54]. For this calculation, a much needed parameter, *i.e.* the height or thickness of the columnar stratum is unknown. This is because of the absence of a wide angle reflection responsible for intracolumnar spacing as a consequence of the lack of long-range periodicity along the columnar axis. Nevertheless, we deduced the value of Z by using the alkyl halo (h_a), and it was found to be three. The results indicated that, each slice of the columns has composed of three molecules and this value is consistent with the calculated large lattice area, $S = 877.69$ Å^2 and volume, $V = 3923.29$ Å^3.

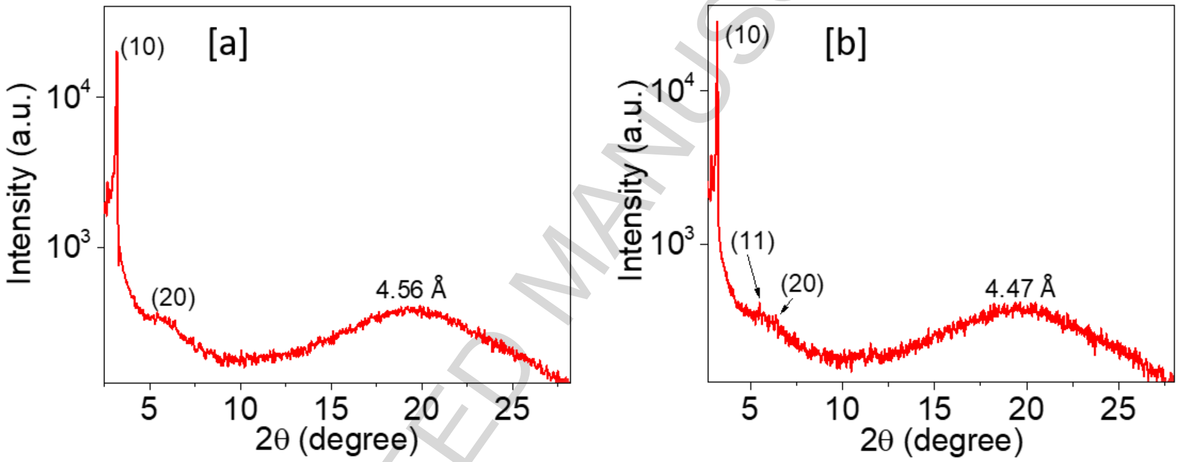

Figure 7. XRD patterns obtained for Col_h phase for **11b** at (a) 123 °C and (b) 125 °C

As mentioned earlier, it is clear that, each columnar stratum of Col_h phase of **11b**, comprises three wedge-shaped molecules. Since tip of these molecules is bearing a polar maleimide group, capable of forming H-bonding, they can assemble comfortably to form a supramolecular disk by means of H-bonded interaction. The resulting H-bond driven macrocyclic structure is depicted in Figure 8. These superstructures form a long-range columnar assemblies in the hexagonal fashion. On the basis of XRD results, we proposed a schematic model for the self-assembly of wedge-shaped maleimide **11b**, as illustrated in Figure 9.

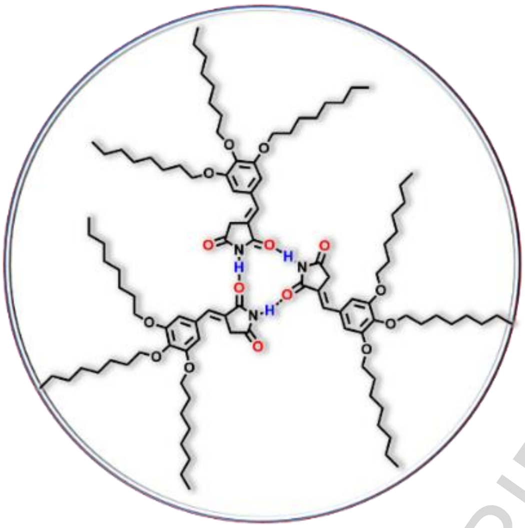

Figure 8. H-bond driven supramolecular disc of **11b**

Table 3. XRD indexation of mesogen **11b**

Compd.	Phase (*T*/℃)	d_{obs} [Å]	d_{cal} [Å]	Miller Indices (*hk*)	Lattice parameter *a* [Å], Lattice area *S* [Å^2], Molecular volume *V* [Å^3]
10b	Col$_h$ (123)	27.61	27.61	(10)	*a* = 31.88
		13.83	15.76	(20)	*S* = 880.24
		4.56 (h_a)			*V* = 4013.9
					Z = 3.2
	Col$_h$ (125)	27.57	26.034	(10)	*a* = 31.83
		16.01	15.91	(11)	*S* = 877.69
		13.44	13.78	(20)	*V* = 3923.29
		4.47 (h_a)			*Z* = 3.1

d_{obs}, observed spacings; d_{cal}, calculated spacings from the lattice parameter *a* for the hexagonal lattice; h_a, alkyl chains correlation peak value; *Z*, number of molecules per columnar unit

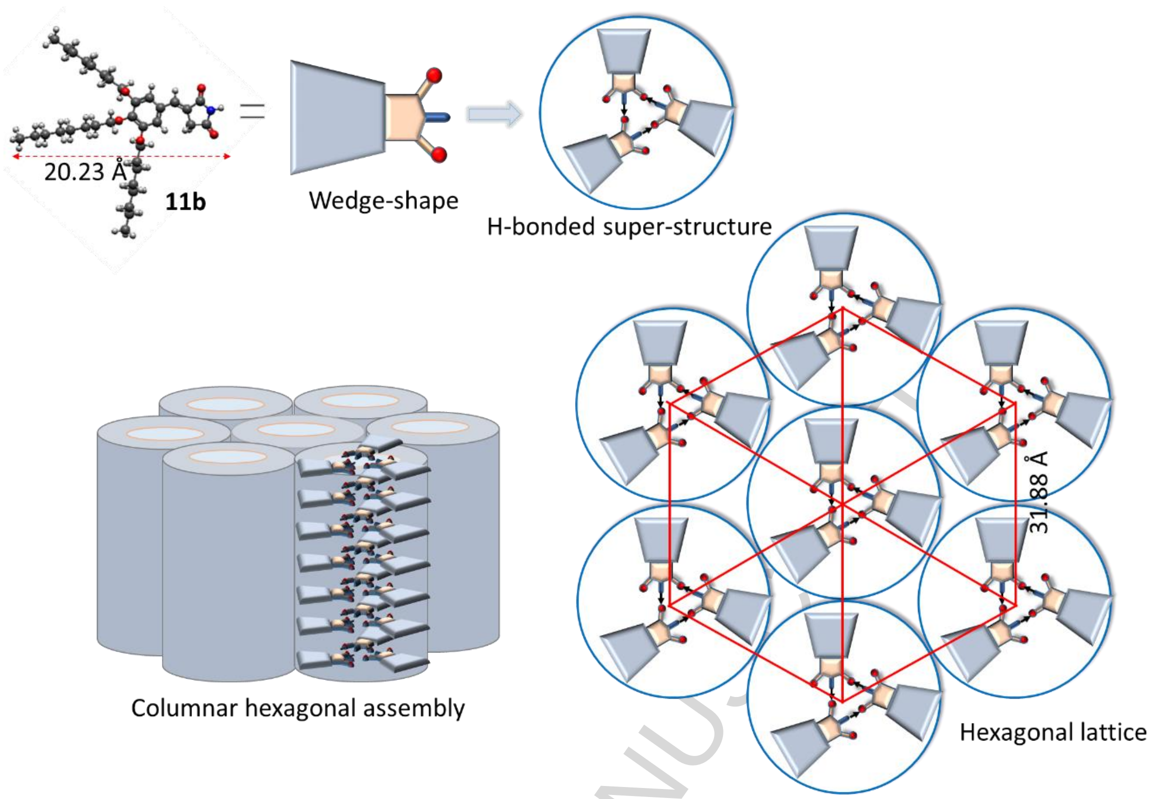

Figure 9. Schematic illustration of columnar hexagonal self-assembly of **11b**

3. Conclusion

In summary, two new series of amphiphilic derivatives with maleimide head group were designed and synthesized. In the new designs, the aromatic core-length and peripheral chain length were rationally varied. Their thermotropic mesomorphism was investigated using standard techniques. It was observed that, the length of hydrophobic segment has significant influence on their LC behaviour. Further, two molecules with tapered-shape have been shown to exhibit a room temperature mesophase with a notable smectic order, irrespective of length of alkyl chains. While, the only midst alkyl member of wedge-shaped derivatives demonstrated an imperative supramolecular columnar phase with hexagonal lattice geometry. From the XRD analysis, we concluded that totally three wedge-shaped molecules occupied in each slice of $\mathrm{Col_h}$ of **11b**, which may be attributed to the possible close-type intermolecular H-bonding through polar maleimide functionality. Conclusively, the showcased results would be the basis for designing new unconventional LC materials for their future applications.

Acknowledgement

The authors are thankful to NITK, Surathkal and SCM group, RRI, Bangalore, India, for providing necessary laboratory facilities. The authors are also grateful to Dr. Vijayaraghavan for recording the NMR spectra, Mrs. K. N. Vasudha for their technical support. VK is grateful to NITK for providing fellowship.

References

[1] G. Meier, E. Sackmann, J.G. Grabmaier, Applications of liquid crystals, Springer Science & Business Media, 2012.

[2] J.W. Goodby, P.J. Collings, T. Kato, C. Tschierske, H.F. Gleeson, P. Raynes, Handbook of liquid crystals, (2014).

[3] L. Wang, D. Huang, L. Lam, Z. Cheng, Bowlics: history, advances and applications, Liq. Cryst. Today. 26 (2017) 85–111.

[4] L. Wang, Q. Li, Photochromism into nanosystems: towards lighting up the future nanoworld, Chem. Soc. Rev. 47 (2018) 1044–1097.

[5] L. Wang, Q. Li, Stimuli-Directing Self-Organized 3D Liquid-Crystalline Nanostructures: From Materials Design to Photonic Applications, Adv. Funct. Mater. 26 (2016) 10–28.

[6] L. Wang, Self-activating liquid crystal devices for smart laser protection, Liq. Cryst. 43 (2016) 2062–2078.

[7] T. Kato, T. Yasuda, Y. Kamikawa, M. Yoshio, Self-assembly of functional columnar liquid crystals, Chem. Commun. (2009) 729–739.

[8] C. Tschierske, Development of structural complexity by liquid-crystal self-assembly, Angew. Chem. Int. Ed. 52 (2013) 8828–8878.

[9] X.-H. Cheng, H.-F. Gao, Hydrogen Bonding for Supramolecular Liquid Crystals, in: Hydrog. Bond. Supramol. Mater. Springer, 2015: pp. 133–183.

[10] T. Kato, N. Mizoshita, K. Kanie, Hydrogen-bonded liquid crystalline materials: Supramolecular polymeric assembly and the induction of dynamic function, Macromol. Rapid Commun. 22 (2001) 797–814.

[11] T. Kato, J. Uchida, T. Ichikawa, T. Sakamoto, Functional Liquid Crystals towards the Next Generation of Materials, Angew. Chem. Int. Ed. 57 (2018) 4355–4371.

[12] L. Wang, A.M. Urbas, Q. Li, Nature-Inspired Emerging Chiral Liquid Crystal Nanostructures: From Molecular Self-Assembly to DNA Mesophase and Nanocolloids, Adv. Mater. (2018) 1801335.

[13] P.J. Jessy, S. Radha, N. Patel, Morphological, optical and dielectric behavior of chiral nematic liquid crystal mixture: Study on effect of different amount of chirality, J. Mol. Liq. 255 (2018) 215–223.

[14] H. Nemati, S. Liu, A. Moheghi, V.P. Tondiglia, K.M. Lee, T.J. Bunning, D.-K. Yang, Enhanced reflection band broadening in polymer stabilized cholesteric liquid crystals with negative dielectric anisotropy, J. Mol. Liq. (2018).

[15] L. Wang, H.K. Bisoyi, Z. Zheng, K.G. Gutierrez-Cuevas, G. Singh, S. Kumar, T.J. Bunning, Q. Li, Stimuli-directed self-organized chiral superstructures for adaptive windows enabled by mesogen-functionalized graphene, Mater. Today. 20 (2017) 230–237.

[16] G. Barbero, W. Zheng, B. Zappone, Twist transitions and force generation in cholesteric liquid crystal films, J. Mol. Liq. 267 (2018) 242–248.

[17] K. Liu, D. Pesce, C. Ma, M. Tuchband, M. Shuai, D. Chen, J. Su, Q. Liu, J.Y. Gerasimov, A. Kolbe, Solvent-Free Liquid Crystals and Liquids Based on Genetically Engineered Supercharged Polypeptides with High Elasticity, Adv. Mater. 27 (2015) 2459–2465.

[18] L.A. Bulavin, L.N. Lisetski, S.S. Minenko, A.N. Samoilov, V.V. Klepko, S.I. Bohvan, N.I. Lebovka, Microstructure and optical properties of nematic and cholesteric liquid crystals doped with organo-modified platelets, J. Mol. Liq. 267 (2018) 279–285.

[19] L. Wang, D. Chen, K.G. Gutierrez-Cuevas, H.K. Bisoyi, J. Fan, R.S. Zola, G. Li, A.M. Urbas, T.J. Bunning, D.A. Weitz, Optically reconfigurable chiral microspheres of self-organized helical superstructures with handedness inversion, Mater. Horiz. 4 (2017) 1190–1195.

[20] R. Kleppinger, C.P. Lillya, C. Yang, Discotic liquid crystals through molecular self-assembly, J. Am. Chem. Soc. 119 (1997) 4097–4102.

[21] E. Beltrán, E. Cavero, J. Barberá, J.L. Serrano, A. Elduque, R. Giménez, Self-Assembly in Helical Columnar Mesophases and Luminescence of Chiral 1H-Pyrazoles, Chem. Eur. J. 15 (2009) 9017–9023.

[22] H. Gallardo, M. Ferreira, A.A. Vieira, E. Westphal, F. Molin, J. Eccher, I.H. Bechtold, Columnar mesomorphism of bent-rod mesogens containing 1, 2, 4-oxadiazole rings, Tetrahedron. 67 (2011) 9491–9499.

[23] H. Blanco, V. Iguarbe, J. Barberá, J.L. Serrano, A. Elduque, R. Giménez, Supramolecular Columnar Liquid Crystals with Tapered-Shape Simple Pyrazoles Obtained by Efficient Henry/Michael Reactions, Chem. Eur. J. 22 (2016) 4924–4930.

[24] L.-X. Guo, Y.-H. Liu, L. Wang, M. Wang, B.-P. Lin, H. Yang, Hydrogen-bonding induced melamine-core supramolecular discotic liquid crystals, J. Mater. Chem. C. 5 (2017) 9165–9173.

[25] Y. Ren, R. Zhang, C. Yan, T. Wang, H. Cheng, X. Cheng, Self-assembly, AIEE and mechanochromic properties of amphiphilic α-cyanostilbene derivatives, Tetrahedron. 73 (2017) 5253–5259.

[26] M.J. Krische, J.-M. Lehn, The utilization of persistent H-bonding motifs in the self-assembly of supramolecular architectures, in: Mol. Self-Assem. Org. Inorg. Approaches, Springer, 2000: pp. 3–29.

[27] T. Kato, N. Mizoshita, K. Kishimoto, Functional liquid-crystalline assemblies: self-organized soft materials, Angew. Chem. Int. Ed. 45 (2006) 38–68.

[28] R. Kleppinger, C.P. Lillya, C. Yang, Self-Assembling Discotic Mesogens, Angew. Chem. Int. Ed. Engl. 34 (1995) 1637–1638.

[29] F. Würthner, S. Yao, B. Heise, C. Tschierske, Hydrogen bond directed formation of liquid-crystalline merocyanine dye assemblies, Chem. Commun. (2001) 2260–2261.

[30] S. Moyano, J. Barberá, B.E. Diosdado, J.L. Serrano, A. Elduque, R. Giménez, Self-assembly of 4-aryl-1 H-pyrazoles as a novel platform for luminescent supramolecular columnar liquid crystals, J. Mater. Chem. C. 1 (2013) 3119–3128.

[31] S. Yagai, Y. Goto, X. Lin, T. Karatsu, A. Kitamura, D. Kuzuhara, H. Yamada, Y. Kikkawa, A. Saeki, S. Seki, Self-Organization of Hydrogen-Bonding Naphthalene Chromophores into J-type Nanorings and H-type Nanorods: Impact of Regioisomerism, Angew. Chem. Int. Ed. 51 (2012) 6643–6647.

[32] S. Yagai, Y. Goto, T. Karatsu, A. Kitamura, Y. Kikkawa, Catenation of Self-Assembled Nanorings, Chem. Eur. J. 17 (2011) 13657–13660.

[33] Y. Kamikawa, M. Nishii, T. Kato, Self-Assembly of Folic Acid Derivatives: Induction of Supramolecular Chirality by Hierarchical Chiral Structures, Chem. Eur. J. 10 (2004) 5942–5951.

[34] K. Kanie, M. Nishii, T. Yasuda, T. Taki, S. Ujiie, T. Kato, Self-assembly of thermotropic liquid-crystalline folic acid derivatives: hydrogen-bonded complexes forming layers and columns J. Mater. Chem. 11 (2001) 2875–2886.

[35] K. Kanie, T. Yasuda, S. Ujiie, T. Kato, Thermotropic liquid-crystalline folic acid derivatives: supramolecular discotic and smectic Chem. Commun. (2000) 1899–1900.

[36] S.H. Seo, J.H. Park, G.N. Tew, J.Y. Chang, Thermotropic liquid crystals of 1H-imidazole amphiphiles showing hexagonal columnar and micellar cubic phases, Tetrahedron Lett. 48 (2007) 6839–6844.

[37] O.N. Kadkin, J. Tae, S.Y. Kim, E.H. Kim, E. Lee, M.-G. Choi, Liquid crystal phases generated by supramolecular self-assembly of biforked amphiphilic imidazoles, Liq. Cryst. 36 (2009) 1337–1347.

[38] J.-H. Park, M.-S. Kim, S.-H. Seo, J.-Y. Chang, Synthesis, self-assembly, and catalytic activity of 1H-imidazole amphiphiles, Bull. Korean Chem. Soc. 32 (2011) 2193–2198.

[39] K.E. Maly, C. Dauphin, J.D. Wuest, Self-assembly of columnar mesophases from diaminotriazines, J. Mater. Chem. 16 (2006) 4695–4700.

[40] M. Suarez, J.-M. Lehn, S.C. Zimmerman, A. Skoulios, B. Heinrich, Supramolecular liquid crystals. Self-assembly of a trimeric supramolecular disk and its self-organization into a columnar discotic mesophase, J. Am. Chem. Soc. 120 (1998) 9526–9532.

[41] T. Kato, Y. Kamikawa, Hydrogen-Bonded Systems: Discrete Defined Aggregates by Intermolecular H-Bonding, Amides, Carboxylic Acids, and Heterocycles, Handb. Liq. Cryst. (2014) 1–28.

[42] T.N. Ahipa, A.V. Adhikari, New cyanopyridone based luminescent liquid crystalline materials: synthesis and characterization, Photochem. Photobiol. Sci. 13 (2014) 1496–1508.

[43] D.R. Vinayakumara, H. Ulla, S. Kumar, A. Pandith, M.N. Satyanarayan, D.S. Rao, S.K. Prasad, A.V. Adhikari, Hydrogen bond-driven columnar self-assembly of electroluminescent D–A–D configured cyanopyridones, J. Mater. Chem. C. 6 (2018) 7385–7399.

[44] D.R. Vinayakumara, K. Swamynathan, S. Kumar, A.V. Adhikari, Optoelectronic Exploration of Novel Non-symmetrical Star-shaped Discotic Liquid Crystals Based on Cyanopyridine, New J. Chem. (2018).

[45] D.R. Vinayakumara, H. Ulla, S. Kumar, M.N. Satyanarayan, A.V. Adhikari, New Fluorescent Columnar Mesogens Derived from Phenanthrene-Cyanopyridone Hybrids for OLED Application, Mater. Chem. Front. (2018).

[46] K. Tanabe, T. Yasuda, M. Yoshio, T. Kato, Viologen-based redox-active ionic liquid crystals forming columnar phases, Org. Lett. 9 (2007) 4271–4274.

[47] S. Maruyama, K. Sato, H. Iwahashi, Room temperature liquid porphyrins, Chem. Lett. 39 (2010) 714–716.

[48] W. Dobbs, L. Douce, B. Heinrich, 1-(4-Alkyloxybenzyl)-3-methyl-1H-imidazol-3-ium organic backbone: A versatile smectogenic moiety, Beilstein J. Org. Chem. 5 (2009).

[49] A.S. Achalkumar, D.S.S. Rao, C.V. Yelamaggad, Non-symmetric dimers comprising chalcone and cholesterol entities: an investigation on structure–property correlations, New J. Chem. 38 (2014) 4235–4248.

[50] J. Mandal, S. Krishna Prasad, D.S. Rao, S. Ramakrishnan, Periodically clickable polyesters: study of intrachain self-segregation induced folding, crystallization, and mesophase formation, J. Am. Chem. Soc. 136 (2014) 2538–2545.

[51] P. Kumar, D.S. Shankar Rao, S. Krishna Prasad, N. Jayaraman, Connector type-controlled mesophase structures in poly (propyl ether imine) dendritic liquid crystals of identical dendrimer generations, J. Polym. Sci. Part Polym. Chem. 55 (2017) 3665–3678.

[52] C.V. Lobo, S.K. Prasad, D.S. Rao, X-ray and dielectric measurements of the smectic-A–hexatic-B transition in bulk and confined geometries, Phys. Rev. E. 69 (2004) 051706.

[53] S. Kumar, Chemistry of discotic liquid crystals: form monomers to polymers, Boca Raton (FL): Taylor and Francis, CRC Press, 2011.

[54] H. Cheng, H. Gao, T. Wang, M. Xia, X. Cheng, Polycatenar bent-shaped liquid crystals with columnar and cubic phases: Synthesis multi-responsive organogels and chemosensors, J. Mol. Liq. 249 (2018) 723–731.

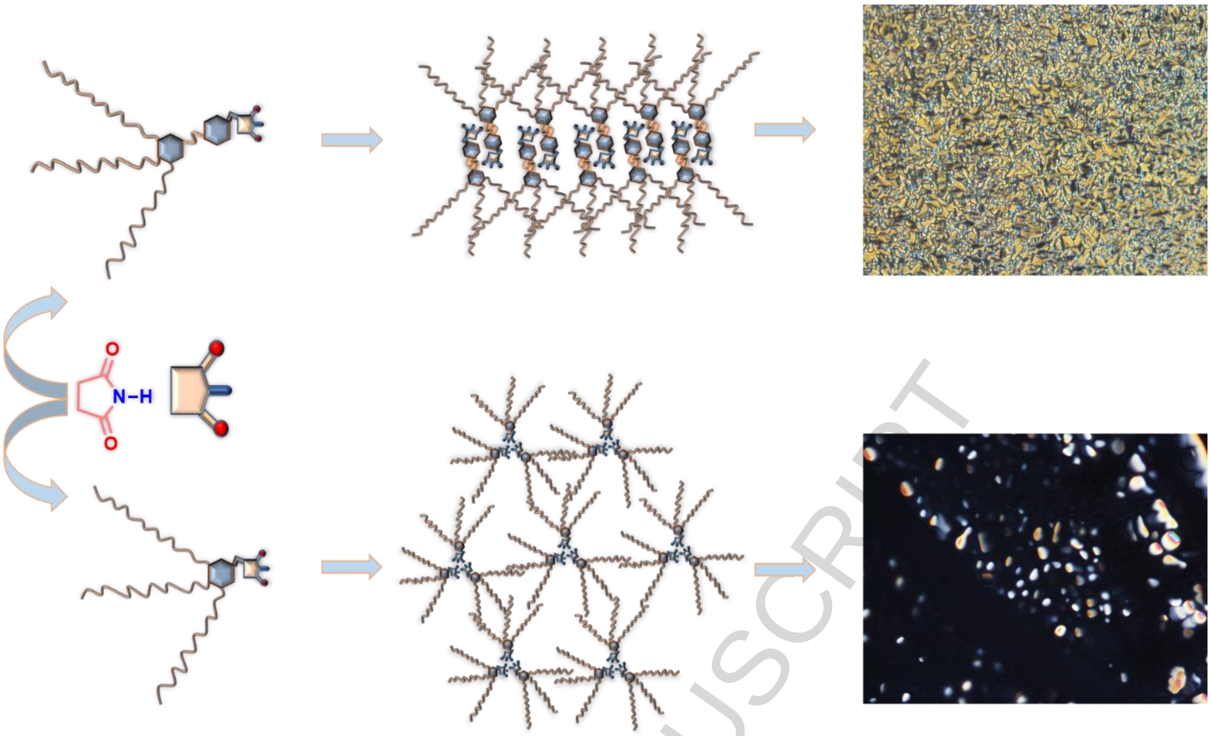

Graphical abstract

Highlights

- New series of tapered and wedge shaped molecules have been designed and synthesized
- Tapered-shaped molecules exhibits stable enantiotropic smectic mesomorphism
- Wedge-structures shown to possess supramolecular columnar mesophase by H-bonding
- The present work mainly emphasizes on the structure-LC property relationship